Effect of fluorine doping on LiCoO$_2$ cathode material: a DFT study

Hatef Yousefi Mashhour [a], Mohammad Mahdi Kalantarian [b*], Afshin Namiranian [a*]

[*]Corresponding Author Emails: kalantarian@gmail.com and m.kalantarian@merc.ac.ir (Mohammad Mahdi Kalantarian), Afshinn@iust.ac.ir (Afshin Namiranian)

[a] Faculty of Physics, Iran university of science and technology, P.O. Box 13114-16846, Tehran, Iran.
[b] *Ceramic Department, Materials and Energy Research Center, P.O. Box 31787-316, Tehran, Iran.*

Abstract

This study employs density functional theory (DFT) in order to investigate the fluorine doping effects on the structural, electrochemical and electrical, properties of LiCoO$_2$ cathode materials for LIBs. The research reveals that fluorine substitution with oxygen can significantly enhance the performance and stability of LiCoO$_2$ in multiple aspects. Investigation show that the fluorine doping results in n-type doping and Fermi level increases in electron density of states, which may enhance the electrical conduction. The substitution of fluorine modifying the cycling life of battery and improves the structural stability by suppressing the expansion rate of volume and increasing the lattice parameter along the c-axis during full delithiation. The findings demonstrate that the fluorine doping improves the structural stability of LiCoO$_2$ by decreasing volume shrinkage during the delithiation. Accordingly, the study identifies the most stable fluorine substitution site, located furthest from the lithium layer. Consistent results from calculations using different approaches (internal and Fermi energy) and methods (GGA and GGA+U) confirm that LiCoO$_{2-x}$F$_x$ exhibits lower voltage compared to LiCoO$_2$, making it desirable for electrolyte tolerance and prolonged battery lifetime. Evaluation of electrical properties demonstrates that the fluorine doping enhances the electrical conductivity of LiCoO$_2$ by reducing the band gap and charge carrier transfer barrier (CCTB). The examination of intrinsic and extrinsic band gaps, as well as Delta and CCTB approaches, consistently reveals that LiCoO$_{2-x}$F$_x$ exhibits a lower band gap and CCTB, indicating improved rate-capability and electrical conductivity.

Key words: Li-ion batteries, Cathode materials, Density Functional Theory, Density of States, Doping

1. INTRODUCTION

In the present era, lithium-ion batteries (LIBs) have emerged as the predominant power source for portable electric devices (Kim, Song, Son, Ono, & Qi, 2019). However, the current commercially utilized cathode materials suffer from limited reversible capacity, exemplified by Layered LiNi$_{1/3}$Mn$_{1/3}$Co$_{1/3}$O$_2$ (150-160 mAhg-1), LiCoO$_2$ (~140 mAhg^{-1}), olivine LiFePO$_4$ (~160 mAhg^{-1} and spinel LiMn$_2$O$_4$ (~120 mAhg^{-1}),) (Barkholtz et al., 2019; Blomgren, 2016; Ellis, Lee, & Nazar, 2010). This constraint poses a significant obstacle to the advancement of Li-ion cathode materials.

Among the existing cathode materials, lithium cobalt oxide (LiCoO$_2$) is widely employed in the current LIB industry (Mizushima, Jones, Wiseman, & Goodenough, 1980; Nagaura, 1990). Its layered structure offers advantages such as satisfactory energy and power densities, high rate capacity, and reasonable reversibility. Nonetheless, the structural stability of LiCoO$_2$ cathodes during charging and discharging poses a substantial challenge. Recent investigations

have revealed notable lattice expansion along the c axis during delithiation, while the contraction rate reaches up to just 10% for complete deintercalation (G. Amatucci, Tarascon, & Klein, 1996; Momeni, Mashhour, & Kalantarian, 2019; Reimers & Dahn, 1992). This non-uniform variation of lattice exceeds the elastic strain tolerance of cobalt oxides, which is approximately 0.1%, resulting in mechanical fractures that adversely affect battery capacities over prolonged operation periods (Dokko et al., 2000; Thackeray, 1995; H. Wang, Jang, Huang, Sadoway, & Chiang, 1999).

To address this issue, substitutional doping sites of Co with various transition metals has been explored to improve the structural stability of LiCoO$_2$ during the deintercalation process (Fergus, 2010; Jones, Rossen, & Dahn, 1994; Kobayashi et al., 2000; Needham, Wang, Liu, Drozd, & Liu, 2007). Notably, the substitution of Co species with Mg and La has demonstrated effective retention of the layered structure, suppression of phase transitions during Li lithiation/delithiation, and significant improvements in performance of cycling for LIBs (Zhu et al., 2014). Materials with doping showed minor capacity fade and

much higher columbic efficiency compared to pristine $LiCoO_2$ (Thirunakaran, Kim, & Yoon, 2014). Conversely, doping with V, Cr, Mo, and Zr leads to a deficient $LiCoO_2$ structure and irreversible capacity loss in the initial cycle (Needham et al., 2007).

On the other hand, substitutional doping of oxygen sites with anionic elements, such as halogens, has received not as much of attention, while it can be promising strategy. Studies have indicated that fluorine substitution with oxygen also impacts the structural properties of cobalt and nickel oxides (G. G. Amatucci & Pereira, 2007; Naghash & Lee, 2001). F-doped $LiNiO_2$ was found to remove abrupt changes in distortion of lattice and remarkably improve the cycling life of LIBs (Kubo, Fujiwara, Yamada, Arai, & Kanda, 1997). Also, $LiNi_xCo_yMn_{1-x-y}O_{2-z}F_z$ ($0 \leq z \leq 0.1$) compounds show improved structural stability without phase transitions during deintercalation, demonstrating excellent cycling performance and rate capacity compared to fluorine-free compounds (Lee et al., 2015).

Utilization of DFT in battery research has revolutionized the field by providing a influential tool for the rational characterization and design of materials (Cohen, Mori-Sánchez, & Yang, 2011; Guillén-López, Espinosa-Torres, Cuentas-Gallegos, Robles, & Muñiz, 2018; Perdew et al., 2017; Ullah, Majid, & Rani, 2018). Its ability to predict material properties, investigate electrochemical processes, and analyze interfaces have significantly accelerated the development of high-performance batteries. By combining theoretical predictions with experimental validation, researchers can drive the discovery of next-generation battery technologies, leading to more efficient, longer-lasting, and safer energy storage devices. (Assat & Tarascon, 2018; A. Wang, Kadam, Li, Shi, & Qi, 2018; Yu & Manthiram, 2018)

In this study, we investigate the effects of fluorine substitution at oxygen sites in $LiCoO_2$ (hereinafter call LCO) systems using density functional theory (DFT) calculations. Our analysis encompasses variance of lattice during delithiation, electrode voltage, electronic state, and its influence on rate capability. Through these investigations, our goal is achieving a better understanding of the implications of fluorine substituted $LiCoO_{2-x}F_x$ (hereinafter call LCOF) cathode materials.

2. Methodology

In this work all of the calculations were performed by employing full- potential linear augmented plane wave (FP-LAPW) method as used in the WIEN2K code (Blaha, Schwarz, Madsen, Kvasnicka, & Luitz, 2001) by the frame-work of DFT.

Using PBE-GGA full relaxation was performed.

Also, we applied GGA plus an on-site Coulomb self-interaction correction potential (U^{SIC}) (hereinafter called GGA+U) to obtain more accurate electrical properties, for more comprehension. The U value was calculated to be equal to 5.87 eV for Co atom int the LCO structure, which it was equal to the used U value in literature, 6 eV (M. M. Kalantarian, Asgari, Capsoni, & Mustarelli, 2013; Meng & Arroyo-de Dompablo, 2009, 2012). The calculations were carried out as ferromagnetic (FM) in GGA and GGA+U methods.

For each atom, in the Wien2k code, a sphere radius around it should be considered. It is called as muffin tin radius, and denoted as RMT. The RMT values of 1.84, 1.76, 1.42 and 1.35 a.u. were used for Co, Li, O, and F atoms, respectively.

In this study, hexagonal structured with the $R\bar{3}m$ space group was considered as initial structure of $LiCoO_2$ cathode material. The primitive structure (atomic positions and structural characteristics) was taken from ref. (Akimoto, Gotoh, & Oosawa, 1998). For the structure, calculated integrals were over the Brillouin zone with k-points based on 11×11×2 Monkhorst–Pack (MP) (Monkhorst & Pack, 1976) mesh for hexagonal structure.

3. RESULTS AND DISSCUSSION
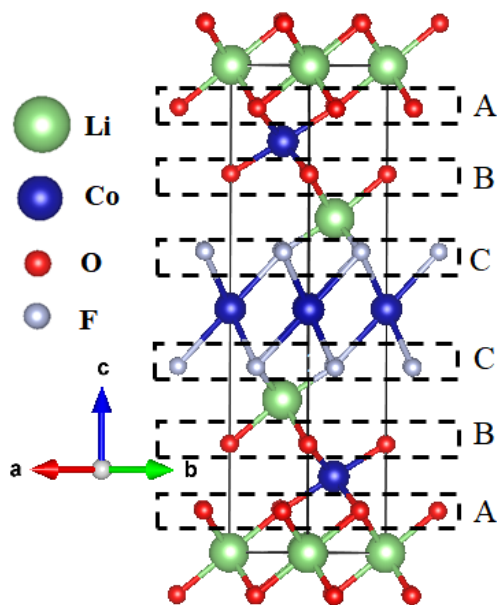
3.1. Structural properties and structural stability

Figure 1. Schematics of intercalated (unite cell) structures of the assessed $LiCoO_{2-x}F_x$ cathode materials with demonstrated symmetric substitution sites A, B, and C.

In layered LCO cathode material, lithium atoms and transition metal are positioned in octahedral positions in the evaluated hexagonal structures. There are three unit formulas in each cell. The three parallel planes M, O, and Li make up the material structure, and each atom is arranged into a hexagonal shape. Lithium diffusion is aided by this formation. All of the planes are parallel to the c-axis, since the c-axis is crucial for our considerations. Accordingly, in order to substitute the fluoride with oxygen sites there would be three symmetric sites denoted as A, B, and C. We calculated the substitution of each site and find the energies and forces. The most stable with low amount of forces and energies was found in site of C. Figure 1 illustrates the structure of $LiCoO_{2-x}F_x (x=\frac{2}{3})$ and the mentioned atomic sites for fluorine. It is equal to 12.6 %wt of F-doping and about 16.6 of atomic percentage.

The calculated structures in their lithiated and delithiated states, as well as the changes in the parameters following Li extraction, are shown in Table 1. By noticing the volume cells, it can be concluded that doping caused about 4% volume increase which is mostly effected by the increasing of c axis. As expected, axis c can tolerate the most shrinkage. A stable structure for this cathode material during charge/discharge is predicted by considering the maximum shrinkage of the cell volume after delithiation (structure remains stable in less than 10% change (M. M. Kalantarian, Asgari, & Mustarelli, 2013)). According to Table 1, in terms of volume shrinkage and subsequently the structural stability, fluorine doping not only does not harm the structure but also make structure a little more stable.

TABLE 1. Calculated structural data for delithiated (Delith.) and lithiated (Lith.) $LiCoO_2$ and $LiCoO_{2-x}F_x$ (per Angstrom), structural changes in percent. In the table x is related column value and $\Delta x/x$ is equal to (x delithiation – x lithiation)/ x lithiation.

Material		a	c	Vol.
LiCoO₂	Lith.	2.85	14.16	99.89
	Delith..	2.84	13.67	95.58
	Δx/x(%)	-0.35	-3.46	-4.31
LiCoO₂₋ₓFₓ	Lith.	2.81	15.22	104.04
	Delith.	2.85	14.15	99.83
	Δx/x(%)	1.6	-7.0	-4.0

3.2. Cell voltages

The calculated voltages obtained from two distinct approaches, namely internal and Fermi (Haghipour, Momeni, Yousefi Mashhour, & Kalantarian, 2022)

energy, and produced by the GGA and GG+U methods are shown in Table 2. The main idea of Fermi energy approach is to replace Fermi energy changes with internal energy changes. This method considers the change of Fermi level during the delithiation process. According to the results all approximations and approaches predict that $LiCoO_2$ has the higher voltage and $LiCoO_{2-x}F_x$ has the lower voltage. However, in such a range of cell voltages, the lower value is more desirable regarding electrolyte voltage tolerance.

TABLE 2. Obtained reaction voltages (V) calculated in GGA/+U methods of the evaluated materials, resulted from Fermi and Internal energy approaches.

Material	Voltage (V)			
	Internal		Fermi	
	GGA	GGA+U	GGA	GGA+U
LiCoO₂	3.36	3.78	3.53	3.43
LiCoO₂₋ₓFₓ	3.44	3.66	3.17	3.13

3.3. Electrical properties

By studying calculated DOS diagrams, here, we evaluate the Electrical properties, i.e. rate-capability and band-gap, of the considered materials. We used two main methods for each property to assess the band-gap (BG) and the electrical rate-capability of each material. We report the BG by using the density of states (DOS) diagrams to show the intrinsic (ILBG) and extrinsic (ELBG) bands. The electrical rate-capability was examined using two approaches called as Delta (M. M. Kalantarian, Mashhour, & Barjini, 2020) and CCTB (charge carrier transfer in DOS bands) (Yousefi-Mashhour & Kalantarian, 2021).

Intrinsic and extrinsic band gap

By noticing the resulted *3d* bands as donor and acceptor, we have established that there should be two kinds of BG, i.e. intrinsic- and extrinsic-like BG (ELBG and ILBG, respectively) (M. Kalantarian & Yousefi Mashhour, 2019; M. M. Kalantarian, Mashhour, et al., 2020; Momeni et al., 2019). The BG depends on the spin of each electron, which is a natural property of the electron. Therefore, we have to look at the spin-up and -down of a material separately when we evaluate the BG. The lower energy is more desirable, so the lower BG is the dominant value (M. M. Kalantarian, Mashhour, et al., 2020). For each pair of structures of a material, one with intercalation and one without, the higher BG value determines the electron transfer (M. M. Kalantarian, Mashhour, et al., 2020). So, we first compare the spin-down values of

the delithiated and lithiated structures, and we report the higher one as the spin-down BG of the pair.

In Figure 2, ILBG values of the considered materials are shown in DOS diagram calculated with GGA. Also, resulted ILBGs are given in Table 3. Accordingly, both approximations predicted that LCOF has better conductivity (lower ILBG) than LCO.

Evaluation of ELBG is usually more significant than ILBG, at least for electrode materials (Hatef Yousefi-Mashhour, 2023).

As far as the extrinsic BG (ELBG) was considered as the electrical conductivity criterion, according to Table 4, both approximations show that LCOF has the superiority over LCO and its electrical conductivity is much better. This indicates that the F-doping of LCO has significant modification on electrical conductivity.

TABLE 3. Calculated ILBG for the evaluated LCO and LCOF materials by GGA/+U approaches. The controlling BG (Ctr.) are shown in the right column.

method	electrode	spin-up		spin-down		Ctr.
		int.	deint.	int.	deint.	
GGA	$LiCoO_2$	8.7	11.6	8.7	9.9	9.9
	$LiCoO_{2-x}F_x$	8.3	5.1	8	7.9	8
GGA+U	$LiCoO_2$	6.9	0	8.2	9.5	6.9
	$LiCoO_{2-x}F_x$	4.1	7.3	4.2	6.5	6.5

TABLE 4. Calculated ELBG for the evaluated materials by GGA/+U approaches. The controlling BGs (Ctr.) are shown in the right column.

method	material	spin-up		spin-down		Ctr.
		int.	deint.	int.	deint.	
GGA	$LiCoO_2$	1.2	1.3	1.2	0	1.2
	$LiCoO_{2-x}F_x$	1.2	1	0.4	0	0.4
GGA+U	$LiCoO_2$	6.9	0	2.4	1.7	2.4
	$LiCoO_{2-x}F_x$	4.1	7.3	0	0.2	0.2

Electrical rate-capability

We used two main approaches to assess each material's electrical rate-capability , which are Delta (M. M. Kalantarian, Mashhour, et al., 2020; Momeni et al., 2019) and CCTB (Yousefi-Mashhour & Kalantarian, 2021; Yousefi-Mashhour, Namiranian, & Kalantarian, 2023). The Delta method compares the difference between the intrinsic conduction/valence bands of the structures with and without intercalation, which are called ΔCB/ΔVB (M. M. Kalantarian, Mashhour, et al., 2020; Momeni et al., 2019). This difference indicates the rate-capability criterion. We

have to consider the spin-up and spin-down separately and choose the lowest value among the Delta results as the dominant one. The other method, called CCTB, which is based on how the charge carriers transfer in the density of states (DOS) bands (Yousefi-Mashhour & Kalantarian, 2021; Yousefi-Mashhour et al., 2023). In the both methods, we have to align the Fermi level in the structures with and without intercalation, which shows the behavior of the semiconductor junction.
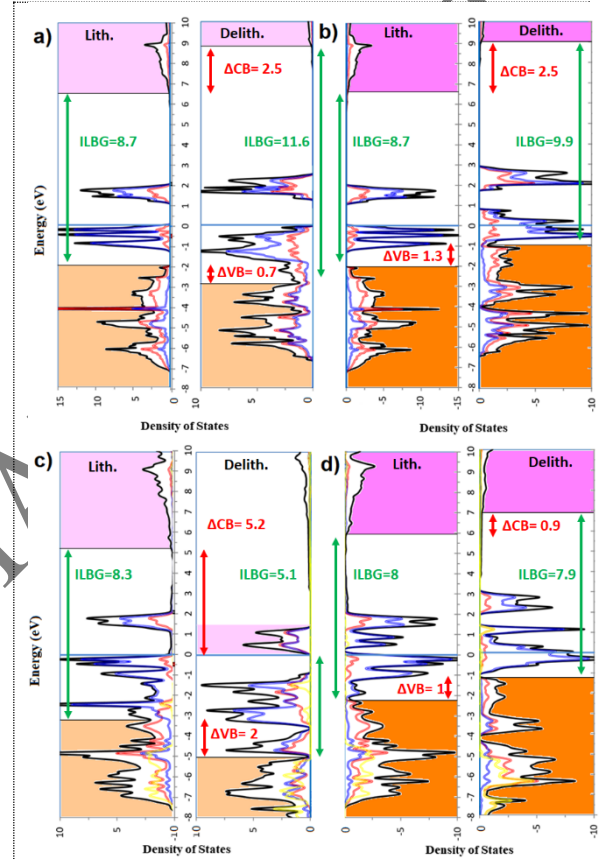

Figure 2. DOS diagrams calculated for intercalated and deintercalated structures via GGA, spin-up, spin-down of a-b) $LiCoO_2$, c-d) $LiCoO_{2-x}F_x$. The intrinsic bands are colored. ILBG, and ΔCB/VB values are shown in the diagrams. The pink and orange colored bands are intrinsic conduction and valance bands, respectively. The lower value among delta values becomes the governing value of the electrode. The Fermi levels set to zero and are aligned for each reacted-unreacted joint structure. The light and dark colors are for spin –up and –down, respectively.

Delta approach

Figure 2 illustrates DOS diagram in view of the Delta approach for GGA method for the considered cathodes. The resulted Delta values for both calculation methods as well as the governing values

are shown in Table 5. According to the table and making comparison by its resulted values between these two electrode materials, our calculations show that, as far as intrinsic rate-capability criterion is considered, both materials are in the same range and show suitable rate capability.

TABLE 5. Calculated values of the Delta criterion via GGA, per eV. The governing (Gvr.) value is the lowest amount in each row.

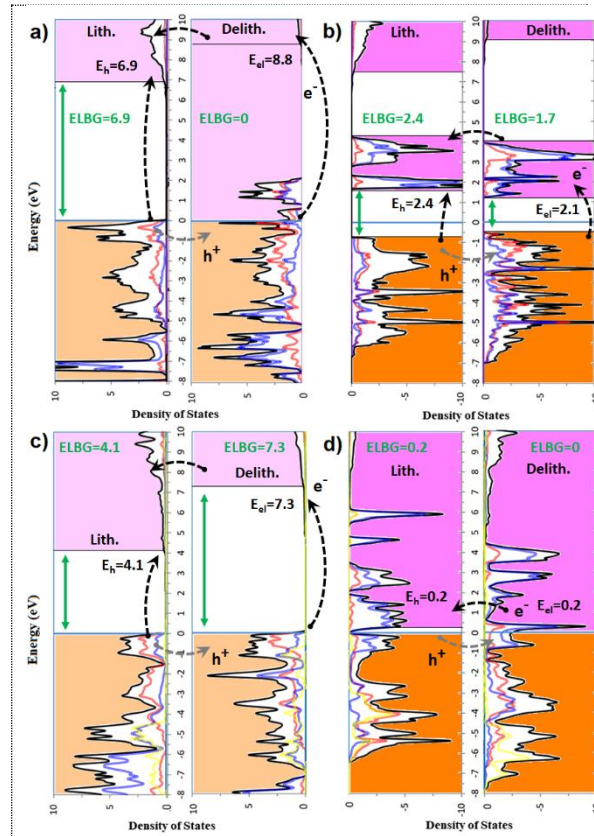| Method	Material	ΔCB		ΔVB		Gvr.
		up	dn	up	dn	
GGA	**LiCoO$_2$**	2.2	2.5	0.7	1.3	0.7
	LiCoO$_{2-x}$F$_x$	5.2	0.9	2	1	0.9

Figure 3. Calculated DOS diagrams via GGA+U for the deintercalated and intercalated structures spin –up and spin-down of a-b) LiCoO$_2$, c-d) LiCoO$_{2-x}$F$_x$. Path of the electron-hole and electron transfer is shown by black and gray arrow, respectively. The generated bands by *3d*-Co orbitals are assumed as acceptor/donor bands. The pink and orange colored bands are intrinsic conduction and valance bands, respectively. The lower value among delta values becomes the governing value of structure. The Fermi levels set to zero and are aligned for each reacted-unreacted joint structure. CCTB values are denoted as E$_{el}$ and E$_h$ for electron and electron-hole

energy, respectively. The light and dark colors are for spin –up and –down, respectively.

Charge carrier transfer in DOS bands (CCTB)

Details of the CCTB approach were explained in Ref. (Yousefi-Mashhour & Kalantarian, 2021). However, here, we explain one case study to recall the concept. Figure 3 displays the DOS diagrams of the studied cathodes computed by the GGA+U method with spin polarization up and down.
Unlike the Delta approach (M. M. Kalantarian, Hafizi Barjini, & Momeni, 2020; M. M. Kalantarian, Mashhour, et al., 2020; Momeni et al., 2019), we use the extrinsic-like bands (ELBs) for CCTB. Therefore, obviously, GGA+U should be more trustworthy. The transfer paths for the electron and electron-hole are indicated in Figure 3 by the black and gray dash-line arrows, respectively.

We can explain the CCTB idea with an example. Figure 3c shows the junction between the structures with and without intercalation (reacted and unreacted) for the spin-up LCOF cathode material, which we calculated using GGA+U. An electron from the valence band of the unreacted structure, COF, can cross the junction and conduct only if the two structures have overlapping electron states in DOS. The electron needs an energy of 7.3 eV to overcome the barrier. However, if we look at Figure 3b, we can see that both structures have overlapped *3d* bands that can help the electron to conduct easily. Therefore, the electron only needs 2.2 eV to overcome the gap barrier and participate in conduction.
As for the electron-hole transfer, we can see from Figure 3b that when an electron has an energy of 2.4 eV. It goes to the conduction band of the intercalated structure and leaves an electron-hole in the valence band. The electron-hole can then move to the valence band of the unreacted structure because these two bands have an overlap. For having a better explanation and information please see Ref. (Yousefi Mashhour & Kalantarian, 2021).
The method gives four values to each electrode, where two of them show how an electron (spin-up and -down) and the other two show how an electron-hole (spin-up and -down) can transfer through junctions. The lowest number is the governing one in this method, because a lower barrier is better. The governing numbers are used to compare the electrodes and see how good they are for the rate-capability. Table 6 shows all and dominant numbers of CCTB method for the electrodes that we studied from the DOS diagrams (Figure 3). In the table, E$_h$ is the energy that is required to transfer an electron-hole, and E$_{el}$ is the energy that is required to transfer an electron from

an unreacted to a reacted structure. The lowest energy among the E_{el}/E_h spin-up/down is the criterion value. According to Table 6, CCTB approach predicted that LCOF has the superiority over LCO and it has much higher rate-capability. Generally, as far as considering the CCTB approach, it can be concluded that 12.6% dopant of fluorine can remarkably improve the electrical rate capability of LCO cathode material.

TABLE 6. The calculated required energy values for transferring holes (E_h) and electrons (E_{el}) crossways deintercalated-intercalated junction, gained from DOS diagrams (Figure 3) by different methods for the considered case studies. The values are in eV unit. The lowest value in each row is the criterion value (C.V) (underlined). Also, the major charge carriers (MCC) are shown in the right column.

Method	Material	Spin-up		Spin-down		C.V/MCC
		E_{el}	E_h	E_{el}	E_h	
GGA+U	LiCoO$_2$	8.8	6.9	<u>2.1</u>	2.4	2.1 / el
	LiCoO$_{2-x}$F$_x$	7.3	4.1	<u>0.2</u>	<u>0.2</u>	0.2 / el-h

4. CONCLUSION

In this work, we studied the structural, electrical, and electrochemical properties of LiCoO$_2$ and LiCoO$_{2-x}$F$_x$ cathode materials for LIBs using DFT. We found that fluorine-doping can improve the performance and stability of LiCoO$_2$ in several aspects.

It was revealed that fluorine-doping can improve the structural stability of LiCoO$_2$ by reducing the volume shrinkage after delithiation. We also found that the most stable fluorine substitution site was C, which is the farthest from the lithium layer.

It was shown that fluorine doping can decrease the cell voltage of LiCoO$_2$ by lowering the Fermi level and the internal energy. We calculated the cell voltages using two different approaches, namely internal and Fermi energy, and two different methods, namely GGA and GGA+U. We obtained consistent results that LiCoO$_{2-x}$F$_x$ had a lower voltage than LiCoO$_2$. This makes it more desirable regarding electrolyte tolerance to have a better lifetime of cell.

Evaluations showed that fluorine doping can improve the electrical properties of LiCoO$_2$ by reducing the band gap and the charge carrier transfer barrier (CCTB). We assessed the band gap and the electrical rate-capability using two main methods, namely intrinsic and extrinsic band gap, and Delta and CCTB approaches. We showed that LiCoO$_{2-x}$F$_x$ has a lower band gap and a lower CCTB than LiCoO$_2$, which indicates a better electrical conductivity and rate-capability.

In conclusion, we demonstrated that fluorine doping can be an effective strategy to modify and optimize the

stability and performance of LiCoO$_2$ cathode materials for LIBs. We also provided a comprehensive analysis of the electrochemical, electrical, and structural properties of LiCoO$_2$ and LiCoO$_{2-x}$F$_x$, using DFT. We hope that our study can provide useful insights and guidance for the development and design of novel cathode materials for LIBs.

5. ACKNOWLEDGEMENTS

REFERENCES

Akimoto, J., Gotoh, Y., & Oosawa, Y. (1998). Synthesis and Structure Refinement of LiCoO 2 Single Crystals. *Journal of Solid State Chemistry, 141*(1), 298-302 .

Amatucci, G., Tarascon, J., & Klein, L. (1996). CoO2, the end member of the Li x CoO2 solid solution. *Journal of The Electrochemical Society, 143*(3), 1114 .

Amatucci, G. G., & Pereira, N. (2007). Fluoride based electrode materials for advanced energy storage devices. *Journal of Fluorine Chemistry, 128*(4), 243-262 .

Assat, G., & Tarascon, J.-M. (201 .(^Fundamental understanding and practical challenges of anionic redox activity in Li-ion batteries. *Nature Energy, 3*(5), 373-386 .

Barkholtz, H. M., Preger, Y., Ivanov, S., Langendorf, J., Torres-Castro, L., Lamb, J., . . . Ferreira, S. R. (2019). Multi-scale thermal stability study of commercial lithium-ion batteries as a function of cathode chemistry and state-of-charge. *Journal of Power Sources, 435*, 226777 .

Blaha, P., Schwarz, K., Madsen, G., Kvasnicka, D., & Luitz, J. (2001). *WIEN2k, An augmented plane wave plus local orbitals program for calculating crystal properties*. Austria: Vienna University of Technology, Austria.

Blomgren, G. E. (2016). The development and future of lithium ion batteries. *Journal of The Electrochemical Society, 164*(1), A501 .٩

Cohen, A. J., Mori-Sánchez, P., & Yang, W. (2011). Challenges for density functional theory. *Chemical Reviews, 112*(1), 289-320 .

Dokko, K., Nishizawa, M., Horikoshi, S., Itoh, T., Mohamedi, M., & Uchida, I. (2000). In Situ

Observation of LiNiO2 Single☐Particle Fracture during Li- Ion Extraction and Insertion. *Electrochemical and Solid-State Letters, 3*(3), 125 .

Ellis, B. L., Lee, K. T., & Nazar, L. F. (2010). Positive electrode materials for Li-ion and Li-batteries. *Chemistry of Materials, 22*(3), 691-7.١٤

Fergus, J. W. (2010). Recent developments in cathode materials for lithium ion batteries. *Journal of Power Sources, 195*(4), 939-954 .

Guillén-López, A., Espinosa-Torres, N. D., Cuentas-Gallegos, A. K., Robles, M., & Muñiz, J. (2018). Understanding bond formation and its impact on the capacitive properties of SiW12 polyoxometalates adsorbed on functionalized carbon nanotubes. *Carbon, 130*, 623-635 .

Haghipour, A., Momeni, M., Yousefi Mashhour, H., & Kalantarian, M. M. (2022). Memory effects' mechanism in the intercalation batteries: the particles' bipolarization. *ACS applied materials & interfaces, DOI: 10.1021/acsami.2c00472* .

Hatef Yousefi-Mashhour, S. S., Samin Hassani, Mohammad Mahdi Kalantarian. (2023). Spin and band-gap in spin-polarized materials for first principal studies. *in press* .

Jones, C. D., Rossen, E., & Dahn, J. (1994). Structure and electrochemistry of Li [sub x] Cr [sub y] Co [sub 1-y] O [sub 2]. *Solid State Ionics;(Netherlands), 68* .

Kalantarian, M., & Yousefi Mashhour, H. (2019). Evaluating electrical properties, band gaps and rate capability of Li2MSiO4 (M= Mn, Fe, Co, Ni) cathode materials using DOS diagrams. *Advanced Ceramics Progress, 5*(3), 30-35 .

Kalantarian, M. M., Asgari, S., Capsoni, D., & Mustarelli, P. (2013). An ab initio investigation of Li 2 M 0.5 N 0.5 SiO 4 (M, N= Mn, Fe, Co Ni) as Li-ion battery cathode materials. *Physical Chemistry Chemical Physics, 15*, 8035-8041 .

Kalantarian, M. M., Asgari, S., & Mustarelli, P. (2013). Theoretical investigation of Li2MnSiO4 as a cathode material for Li-ion batteries: a DFT study. *Journal of Materials Chemistry A, 1*(8), 2847-2855 .

Kalantarian, M. M., Hafizi Barjini, M., & Momeni, M. (2020). Ab Initio Study of AMBO3 (A = Li, Na and M = Mn, Fe, Co, Ni) as Cathode Materials for Li-Ion and Na-Ion Batteries. *ACS Omega, 5*(15), 8952-8961 .

Kalantarian, M. M., Mashhour, H. Y., & Barjini, M. H. (2020). A semi-quantitative approach to

evaluate electrical rate-capability and conductivity of polyanion cathode materials of intercalation batteries using DOS diagrams. *Ceramics International, 46*(10), 15222-15227 .

Kim, T., Song, W., Son, D.-Y., Ono, L. K., & Qi, Y. (2019). Lithium-ion batteries: outlook on present, future, and hybridized technologies. *Journal of Materials Chemistry A, 7*(7), 294.٢٩٦٤-٢

Kobayashi, H., Shigemura, H., Tabuchi, M., Sakaebe, H., Ado, K., Kageyama, H., . . . Morimoto, S. (2000). Electrochemical Properties of Hydrothermally Obtained LiCo1−x Fe x O 2 as a Positive Electrode Material for Rechargeable Lithium Batteries .*Journal of The Electrochemical Society, 147*(3), 960 .

Kubo, K., Fujiwara, M., Yamada, S., Arai, S., & Kanda, M. (1997). Synthesis and electrochemical properties for LiNiO2 substituted by other elements. *Journal of Power Sources, 68*(2), 553-557 .

Lee, S .H., Moon, J.-S., Lee, M.-S., Yu, T.-H., Kim, H., & Park, B. M. (2015). Enhancing phase stability and kinetics of lithium-rich layered oxide for an ultra-high performing cathode in Li-ion batteries. *Journal of Power Sources, 281*, 77-84 .

Meng, Y. S., & Arroyo-de Dompablo, M. E. (2009). First principles computational materials design for energy storage materials in lithium ion batteries. *Energy & Environmental Science, 2*(6), 589-609 .

Meng, Y. S., & Arroyo-de Dompablo, M. E. (2012). Recent Advances in First Principles Computational Research of Cathode Materials for Lithium-Ion Batteries. *Accounts of Chemical Research* .

Mizushima, K., Jones, P., Wiseman, P., & Goodenough, J. B. (1980). LixCoO2 (0< x<-1): A new cathode material for batteries of high energy density. *Materials Research Bulletin, 15*(6), 783-789 .

Momeni, M., Mashhour, H. Y., & Kalantarian, M. M. (2019). New approaches to consider electrical properties, band gaps and rate capability of same-structured cathode materials using density of states diagrams: Layered oxides as a case study. *Journal of Alloys and Compounds, 787*, 738-743 .

Monkhorst, H. J., & Pack, J. D. (1976). Special points for Brillouin-zone integrations. *Physical Review B, 13*(12), 5188-5192 .

Nagaura, T. (1990). Lithium ion rechargeable battery. *Progress in Batteries & Solar Cells, 9*, 209 .

Naghash, A., & Lee, J. Y. (2001). Lithium nickel oxyfluoride (Li1− zNi1+ zFyO2− y) and lithium magnesium nickel oxide (Li1− z (MgxNi1− x) 1+ z O2) cathodes for lithium rechargeable batteries: Part I. Synthesis and characterization of bulk phases. *Electrochimica Acta, 46*(7), 941-951 .

Needham, S., Wang, G., Liu, H.-K., Drozd, V., & Liu, R. (2007). Synthesis and electrochemical performance of doped LiCoO2 materials. *Journal of Power Sources, 174* (۲), ۸۲۸-۸۳۱.

Perdew, J. P., Yang, W., Burke, K., Yang, Z., Gross, E. K., Scheffler, M., . . . Ruzsinszky, A. (2017). Understanding band gaps of solids in generalized Kohn–Sham theory. *Proceedings of the National Academy of Sciences, 114*(11), 2801-2806 .

Reimers, J. N., & Dahn, J. (1992). Electrochemical and in situ X- ray diffraction studies of lithium intercalation in Li x CoO2. *Journal of The Electrochemical Society, 139*(8), 2091 .

Thackeray, M. (1995). Structural considerations of layered and spinel lithiated oxides for lithium ion batteries. *Journal of The Electrochemical Society, 142*(8), 2558 .

Thirunakaran, R., Kim, T., & Yoon, W.-s. (2014). Synthesis and electrochemical characterization on dual-doped LiCoO 2 via green chemistry method for lithium rechargeable batteries. *Journal of Applied Electrochemistry, 44*, 709-718 .

Ullah, A., Majid, A., & Rani, N. (2018). A review on first principles based studies for improvement of cathode material of lithium ion batteries. *Journal of energy chemistry, 27*(1), 21 .۹-۲۳۷

Wang, A., Kadam, S., Li, H., Shi, S., & Qi, Y. (2018). Review on modeling of the anode solid electrolyte interphase (SEI) for lithium-ion batteries. *npj Computational Materials, 4*(1), 1-26 .

Wang, H., Jang, Y. I., Huang, B., Sadoway, D. R., & Chiang, Y. M. (1999). TEM study of electrochemical cycling- induced damage and disorder in LiCoO2 cathodes for rechargeable lithium batteries. *Journal of The Electrochemical Society, 146*(2), 473 .

Yousefi-Mashhour, H., & Kalantarian, M. M. (2021). A theoretical approach to evaluate and understand the electrical properties of the electrode materials of batteries. *Physical Chemistry Chemical Physics, 23*(30), 16013-16022 .

Yousefi-Mashhour, H., Namiranian, A., & Kalantarian, M. M. (2023). A first principle study of structural and electrical properties of novel Li2FeO3/Li2FeO2F Li-ion battery cathode material. *ФІЗИКА НИЗЬКИХ ТЕМПЕРАТУР, 49*(1), 42-49 .

Yousefi Mashhour, H., & Kalantarian, M. M. (2021). A theoretical approach to evaluate and understand the electrical properties of the electrode materials of batteries. *Physical Chemistry Chemical Physics, 23*, 16013-16022 .

Yu, X., & Manthiram, A. (2018). Electrode– electrolyte interfaces in lithium-based batteries. *Energy & Environmental Science, 11*(3), 527-543 .

Zhu ,X., Shang, K., Jiang, X., Ai, X., Yang, H., & Cao, Y. (2014). Enhanced electrochemical performance of Mg-doped LiCoO2 synthesized by a polymer-pyrolysis method. *Ceramics International, 40*(7), 11245-11249 .